https://doi.org/10.5194/egusphere-2022-359
Preprint. Discussion started: 4 July 2022

Upscaling microbial stoichiometric adaptability in SOM turnover: The SESAM Soil Enzyme Steady Allocation Model (v3.0).

Thomas Wutzler[1], Lin Yu[12], Marion Schrumpf[1], and Sönke Zaehle[1]

[1]Max Planck Institute for Biogeochemistry, Hans-Knöll-Straße 10, 07745 Jena, Germany
[2]Centre for Environmental and Climate Science (CEC) at Lund University, Sölvegatan 37, Lund, Sweden

Correspondence: Thomas Wutzler
(twutz@bgc-jena.mpg.de)

Abstract. Understanding the coupling of nitrogen (N) and carbon (C) cycles of land ecosystems, requires understanding microbial element use efficiencies of soil organic matter (SOM) decomposition. Whereas important controls of those efficiencies by microbial community adaptations have been shown at the scale of a soil pore, a simplified representation of those controls is needed at the ecosystem scale. However, without abstracting from the many details, models are not identifiable, i.e. can not be fitted without ambiguities to observations. There is a need to find, implement, and validate abstract simplified formulations of theses processes.

Therefore, we developed the SESAM model as an abstraction of the more detailed soil enzyme allocation model (SEAM) model and tested, whether it can provide the same decadal-term predictions. SEAM explicitly models community adaptation strategies of resource allocation to extracellular enzymes and enzyme limitations on SOM decomposition. It thus provides a scaling from representing several microbial functional groups to a single holistic microbial community. Here we further abstracted the model using quasi-steady-state assumption for extracellular enzyme pools to derive the SESAM model.

SESAM reproduced the priming effect, the SOM banking mechanism, and the damping of fluctuations of carbon use efficiency with microbial competition as predicted by SEAM and other more detailed models. This development is an important step towards more parsimonious representation of soil microbial effects in global land surface models.

1 Introduction

Soil organic matter (SOM) dynamics constitutes a strong link of global nutrient cycles, because microbial decomposer community has a rather strict homeostatic regulation of their stoichiometry (Sterner and Elser, 2002; Zechmeister-Boltenstern et al., 2015). Hence, understanding and properly modeling SOM dynamics is required to understand the linkage of the global element cycles of nitrogen (N) and carbon (C) (Thornton et al., 2007; Janssens et al., 2010; Zaehle and Dalmonech, 2011; Todd-Brown et al., 2012; Xu et al., 2014). The discussion about microbial carbon use efficiency (CUE) the ratio between microbial uptake and microbial growth has received attention in literature (Wieder et al., 2013; Bradford et al., 2016; Hagerty et al., 2018; Liu et al., 2018; Fatichi et al., 2019) as an important predictor for building up SOM stocks. However, there is a discrepancy in detail and scale between process understanding and what is feasible to implement in global models.

https://doi.org/10.5194/egusphere-2022-359
Preprint. Discussion started: 4 July 2022

CUE is an emergent value that depends on microbial traits, such as maintenance requirements, and stoichiometric imbalances of the substrates that microbes feed on (section 2.1.1). At the micro-pore scale, competition between single microbes has been shown to allow for a constrained CUE despite changing stoichiometry of the decomposed SOM. By using a detailed individual-based model Kaiser et al. (2014) showed how the succession of different microbial populations with different substrate preferences sustained high community CUE despite changing substrate stoichiometry.

In a first abstraction step models represent different microbial groups or guilds instead of single microbes (Allison, 2014; Perveen et al., 2014; Huang et al., 2018). This matches the scale of inputs and outputs to the SOM model making it potentially feasible to implement them as submodels in global models. However, for each microbial group properties and parameters have to be determined. The increase of number of model parameters inflates the risk of equifinality, i.e. simulating the observed data for the wrong reasons and renders model-data-integration studies difficult. For example Huang et al. (2018) used 11 microbial related model parameters for each group.

An alternative model abstraction represent a single microbial community with adapting properties by e.g. optimizing microbial growth in the model. This concept was applied in the SEAM model (Wutzler et al., 2017), which was successful in reproducing the simulated patterns of the more group-based SYMPHONY model (Perveen et al., 2014).

In a further model abstraction, the effect of changing CUE can be modeled in conventional pool-based models without explicit microbial community by a growth-adapted humification coefficient and stoichiometry-dependent decomposition rates as in the PRIM model (Guenet et al., 2016). However, such a model cannot represent the changes in decomposition rate with apparent CUE depending on biomass properties (Tang and Riley, 2014).

Hence, there is a need for an model abstraction with fewer detail and fewer parameters that is still able to represent effects of stoichiometry such as priming effects due to mining N from from SOM under N-limitation (Kuzyakov, 2010), and the bank mechanism (Perveen et al., 2014; Wutzler et al., 2017). To meet this need, we present the soil enzyme steady allocation model (SESAM), a further abstraction of the SEAM model (Wutzler et al., 2017).

The SESAM model is intended to capture the longer-term, i.e. decadal dynamics of SOM decomposition and abstracts from short-term dynamics by applying the quasi steady state assumption (Wutzler and Reichstein, 2013) to soil extracellular enzyme pools.

The aim of this paper is to present the SESAM model, show that it can reproduce the predictions of the SEAM model at decadal time scale, and is therefore able to simulate the priming effect due to N mining and the banking mechanism.

2 Methods

2.1 SESAM model

The dynamic Soil Enzyme Steady Allocation Model (SESAM) allows exploring consequences soil microbial stoichiometry for SOM cycling at the soil core to ecosystem scale at decadal time scale. The modeled system are C and N pools in SOM in a volume of soil. Such a system can be a layer of a soil profile or a laboratory incubation. It can be integrated into a larger model that explicitly represents entire soil column and vertical transport.

https://doi.org/10.5194/egusphere-2022-359
Preprint. Discussion started: 4 July 2022

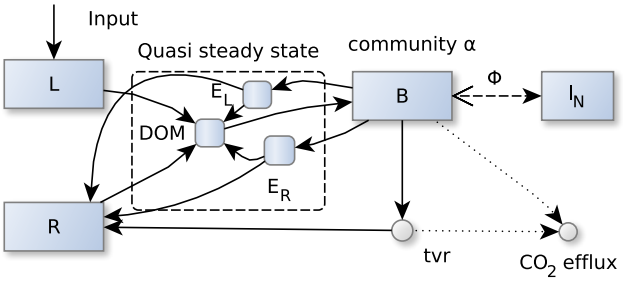

Figure 1. SESAM model structure: microbial biomass B produces enzymes that depolymerize substrate pools (L and R) that differ in their elemental ratios. Microbial community enzyme allocation α determines which part of the microbial community depolymerizes L versus R by producing respective enzymes E_L, E_{LP}, E_R, E_{RP}. Microbes take up dissolved organic matter (DOM) and use it for synthesizing new biomass, new enzymes, or for catabolic respiration. A part of microbial turnover (tvr) adds to the residue pool, another part is mineralized, and another part adds to DOM and is recycled into microbial biomass. Stoichiometric imbalance between DOM and B is resolved by mineralizing the excess element or immobilizing required element (Φ_B) from inorganic N (I) (further detailed in Fig. A1). Boxes correspond to pools, disks to fluxes. Solid lines represent fluxes of both C and N, while dotted and dashed lines represent separate C or N fluxes respectively.

SESAM models several SOM pools containing C and N by differential equations for their mass fluxes. Model drivers are inputs of C and N by plant litter (both above-ground and rhizodeposition), input of inorganic N from deposition and fertilizers, and prescribed root uptake of inorganic N (Table 1).

SESAM represents several SOM by several pools that differ by their stoichiometry, and it represents changes in microbial community structure by changing preferences in degrading specific SOM pools. Litter pool, L is rich in C, residues pool, R is richer in N (Fig. 1, Table 1). While, appendix A provides all the detailed model equations, the following paragraph summarizes most important assumptions. Tab. A1 explains symbols used.

This paper presents model version 3, which in addition to the enzyme steady state assumption differs from published SEAM (Wutzler et al., 2017) by explicitly tracking community composition, α as a state variable, by a modified formula for weighting optimal states near co-limitation, and by a modified calculation of the revenue, which is used in the optimality assumption. The enzymes are assumed to be in steady state, i.e. production of enzymes equals their turnover. This assumptions allows computing the size of the enzyme pools based on other pools, simplify equations, and use fewer parameters in the overall model. The microbial community is assumed to self-organize in ways to optimize growth of the entire community. This involves adjusting relative proportion of groups that preferentially decompose litter and groups that preferentially decompose microbial residues. The enzymes, which are produced in different shares, in turn affect the decomposition of the respective pools.

Decomposition of the litter and residue pools is modeled by reverse Michaelis-Menten kinetics (Schimel and Weintraub, 2003). C/N ratios, β_N, of fluxes are equal to the C/N ratios of the source pools. While The C/N ratios of the substrate pools may change over time due to changing C/N ratio of total influxes to these pools, the of C/N ratios of biomass and enzymes are assumed to be fixed. Total enzyme allocation is modeled as fraction, a_E, of the microbial biomass, B, per time. SESAM

https://doi.org/10.5194/egusphere-2022-359
Preprint. Discussion started: 4 July 2022

Table 1. State variables and model drivers. Values refer to the reference state of the sensitivity analysis. Values are adopted from (Wutzler et al., 2017)

Symbol	Definition	Value	Unit
L	C in litter	109.64	$\mathrm{g\,m^{-2}}$
L_N	N in litter	3.62	$\mathrm{g\,m^{-2}}$
R	C in residue substrate	3336.45	$\mathrm{g\,m^{-2}}$
R_N	N in residue substrate	323.39	$\mathrm{g\,m^{-2}}$
B	microbial biomass C	34.43	$\mathrm{g\,m^{-2}}$
I_N	inorganic N	0.0133	$\mathrm{g\,m^{-2}}$
α_L,α_R	community enzyme allocation	0.5	(-)
$\mathrm{i}_L(t)$	litter C input	400.0	$\mathrm{g\,m^{-2}yr^{-1}}$
$\beta_{N_{\mathrm{i}_L}}(t)$	C/N ratio of plant litter inputs	30	$\mathrm{g\,g^{-1}}$
$i_{I_N}(t)$	inorganic N input	0.7	$\mathrm{g\,m^{-2}yr^{-1}}$
$k_{I_N P}(t)$	inorganic plant N uptake per I_N	100*	$\mathrm{yr^{-1}}$
$u_{I_N,max}(t)$	max inorganic plant N uptake	$=\mathrm{i}_L/\beta_{N_{\mathrm{i}_L}}$	$\mathrm{g\,m^{-2}yr^{-1}}$

* arbitrary high value so that plant uptake is constraint by $u_{I_N,max}(t)$ (eq. A7c)

assumes the DOM pool to be in quasi steady state (Wutzler and Reichstein, 2013) and does not explicitly simulate its changes because the dynamics of the DOM pool is usually much faster than the dynamics of the other pools. Therefore, microbial uptake equals the sum of all influxes to the DOM pool, i.e. decomposition plus part of the enzyme turnover. The microbial carbon balance can be negative, i.e. uptake is smaller than maintenance and enzyme synthesis. In this case biomass declines.

2.1.1 Soil microbial stoichiometry

SESAM assumes that stoichiometry is one of the overarching controls of decadal-scale SOM changes. It assumes that microbial community and development of different SOM stocks adapt to changes in drivers, without the need to explicitly model all the details of this adaptation.

There are three principle ways (Mooshammer et al., 2014b) in how decomposers can adapt to stoichiometric imbalance, i.e. differences in elemental composition between the requirement of feeders and its food (Sterner and Elser, 2002). First, decomposer communities can change their nutrient-use efficiencies (Sinsabaugh et al., 2013) by overflow respiration or mineralizing N. For example, if there is more N in DOM uptake for biomass synthesis than constrained by other ways, such as available C, excess N will be mineralized. Such regulation of nutrient use efficiencies has large consequences for loss of nutrients from the ecosystem (Mooshammer et al., 2014a), plant nutrition and soil plant feedback (Rastetter, 2011) and on carbon sequestration in SOM (Allison, 2014; Wieder et al., 2013). Second, microbes can adapt their stoichiometric requirements. There are possible shifts in community composition between species with lower C/N ratio, such as many bacteria or species with high C/N ratio,

https://doi.org/10.5194/egusphere-2022-359
Preprint. Discussion started: 4 July 2022

such as many fungi (Cleveland and Liptzin, 2007; Xu et al., 2013). However, the range of adjustment is quite constrained. Third, microbial community can alter the stoichiometry of uptake by adapting their preferences of degrading SOM fractions that vary in elemental composition (Moorhead et al., 2012; Li et al., 2021).

The SEAM model (Wutzler et al., 2017) and SESAM assume that a combination of options 1 and 3 is used in a way to optimize growth and option 2 is negligible. Modeled microbial community develops in a way so that different kinds of enzymes are produced in proportion to their revenue, i.e. the decomposition return per unit of limiting element invested into enzyme production. This microbial enzyme allocation strategy performed better in simulation experiments (Wutzler et al., 2017) than a fixed enzyme allocation or stoichiometrically optimized allocation irrespective of the amount of substrate (Moorhead et al., 2012).

While this adaptive single microbial community was a necessary step in the direction to simplify models, SEAM required model parameters for enzyme turnover. These parameters are hard to measure and added complexity to model-data-integration.

2.1.2 Quasi steady state approximation of enzyme dynamics

The SESAM model abstracts from short-term dynamics of enzyme pools in SEAM by assuming that soil extracellular enzyme pools are in quasi steady state (Wutzler and Reichstein, 2013), i.e. pools are at levels where current enzyme production equals enzyme turnover.

It assumes that compared to the intended decadal modeling time scale, the amount of soil extracellular enzymes and the composition of the microbial community approaches a steady state given the annually smoothed inputs and drivers of the modeled system and current SOM stocks. This yields the enzyme states in (1).

$$E_Z^* = \frac{\alpha_Z a_E B}{k_N}, \tag{1}$$

where $Z \in \{R, L\}$ denote enzymes depolymerizing litter and residue substrate. α_Z is the proportion of biosynthesis invested into the respective enzyme (section 2.1.3), a_E is the enzyme production per microbial biomass, B, per time, and k_N is the enzyme turnover time.

This steady state expression is used instead of the explicitly modeled enzyme pool in SEAM to simplify other equations. For example, decomposition of the residue pool now depend on biomass rather than enzyme levels (2).

$$\mathrm{dec}_R = k_R R \frac{E_R}{k_m + E_R} \tag{2a}$$

$$\mathrm{dec}_R^* = k_R R \frac{\alpha_R a_E B}{k_m k_N + \alpha_R a_E B}, \tag{2b}$$

where k_m is the half-saturation constant of the original enzyme-limited decomposition equation.

In the steady state equations, half-saturation k_m, and the enzyme turnover time scale k_N always occur together as product. Hence, they can be replaced by a single parameter k_{mN}.

We further explored two additional potential simplifying model assumptions. First the microbial biomass can be assumed to be in quasi steady state (SteadyB appendix F), and second, neglecting the mass fluxes from microbial biomass to DOM due to

https://doi.org/10.5194/egusphere-2022-359
Preprint. Discussion started: 4 July 2022

production and turnover or organic matter (NoEnzFlux appendix E). Both assumptions yielded models with the same number of parameters. The SteadyB variant had one fewer state variable, however, the representation of biomass B by the solution of a 3rd polynomial yielded no further simplification of model equations compared to SESAM. The NoEnzFlux variant still required the parameters for enzyme production to compute revenues and did not result in model simplification.

2.1.3 Community enzyme allocation α

Enzyme allocation α is defined as the proportion of total enzyme synthesis that is invested into production of a specific enzyme. With SESAM it is computed to be proportional to the revenue, i.e. return per investment. It is normalized to add up to unity (3).

$$\alpha_{Z,Opt} = \frac{\mathrm{rev}_Z}{\sum_\zeta \mathrm{rev}_\zeta} \tag{3}$$

where rev_Z is the revenue from given enzyme Z.

While original SEAM computed both, the return and the investment, for each element $E \in (C, N)$ separately, SESAM computes the revenue based on limitation-weighted return divided by a limitation-weighted investment. The return is determined by the mineralization flux of element E from enzyme action, the investment by amount of E required for enzyme production, and the weight for E is determined by the difference in potential growth constrained by other elements and growth contrained by E (Appendix A4). Compared to the original SEAM formulation this avoids the unreasonable high revenues when the concentration of the limiting element in enzymes is low, e.g. for an extension of SESAM which includes phosphorus limitation.

The return of an element, E for enzyme Z, in SESAM is the flux toward the microbial biomass from decomposition of targeted substrate, S, computed with current steady state enzyme levels, which are determined by current enzyme production (2).

Alternatively to decomposition flux, the microbial uptake flux can define the return. This option is discussed in appendix B, where it is argued, that this does only differ from the simpler decomposition approach in rare cases.

When inserting the steady state revenue into (3), one notices that the revenue in turn depends on current α. Nevertheless explicit formulas for optimal α can be obtained for either assuming C limitation or assuming N limitation. However, situations near co-limitations then pose a problem. At the same substrate levels, a community optimized for C usage is N limited while a community optimized for N usage then is C limited. In SEAM this was prevented by the inertia of explicitly modeled enzyme levels.

In contrast, SESAM does not use these explicit formulas to compute α, but rather computes the revenues based on current instead of the optimum enzyme allocation. To this end it models α as an additional state variable that develops towards an optimal value, α_{Opt}, that can be computed by (3) given the current value of α and corresponding decomposition fluxes and revenues (A13). Since, α represents a property of the microbial community, it changes at the time scale of growth and microbial turnover (A12).

https://doi.org/10.5194/egusphere-2022-359
Preprint. Discussion started: 4 July 2022

2.2 Increased C input simulations

In order to show the ability of SESAM to reproduce the priming effects due to N mining and the banking mechanism, we repeated the CO_2-Fertilization experiment in Wutzler et al. (2017). It studied the effect of increased continuous litter C input on SOM cycling. Such increased C input is expected with elevated atmospheric CO_2 concentration. The simulations started from steady state corresponding to initial litter C input of input 400 $\mathrm{gCm^{-2}yr^{-1}}$, applied 20% increased C inputs during years 10 to 60, and applied initial litter inputs again during the next 50 years. The litter N inputs were kept constant over time, implying an increase in the litter C/N ratio of 20% in annual average litter inputs. Maximum plant uptake rate of inorganic N was set to litter input rate, plus N deposition of 1/200 of litterfall N was compensated by a small leaching rate.

We compared results of the following model variants.

- SEAM: baseline model with explicit representation of extracellular enzymes.
- SESAM: enzyme levels assumed in quasi steady state
- SESAM-NoEnzFlux: additionally neglecting the mass flux of N from microbial biomass to DOM via enzyme production and turnover (appendix E)
- SESAM-SteadyB: additionally microbial biomass assumed in quasi steady state (appendix F)

The derivative of the model variants were implemented in the R programming language (R Core Team, 2021) and solved, i.e. simulated over time, using function lsoda from package deSolve (Soetaert et al., 2009).

2.3 Substrate Pulse simulations

In order to show the ability of SESAM to reproduce the damping of fluctuations of CUE with adapting microbial community, we simulated an incubation experiment. Carbon use efficiency, CUE, is modeled as an emergent property instead of a model parameter. With the Substrate pulse scenario we simulated an experiment similar to the one in (Kaiser et al., 2014), which showed that competition among microbial groups controlled the emergent CUE in a spatially explicit model.

In this experiment microbial community decompose a carbon rich chunk of litter, L, with scenario of varying initial C/N ratio with otherwise very low rate of L input of 40 $\mathrm{gm^{2}yr^{-1}}$ and no export of N out of the system. CUE was computed as synthesis of microbial biomass carbon, i.e. excluding enzyme production and turnover, per carbon taken up.

Simulations were compared between SESAM, which has dynamic enzyme allocation, and a model version where we fixed community enzyme allocation $\alpha_Z = 0.5$ to not dynamically change over time.

We used the same R-based computational setup as in the increased C input simulations.

https://doi.org/10.5194/egusphere-2022-359
Preprint. Discussion started: 4 July 2022

2.4 Sensitivity analysis

In order to explore which parameters most influence the steady state and transient predictions of the increased C input simulation, we performed a global sensitivity analysis using Sobol sensitivity indexes (Saltelli et al., 2008) using method soboltouati in the sensitivity R package using two samples of N = 5000.

For each parameter we prescribed prior distributions of possible parameter values (Table A1). Next, we computed the cumulative probability of initial parameters and sampled cumulative probabilities $\pm 10\%$ around this value. Two samples of cumulative probabilities were used to generate design matrices of the sensitivity method. Next we transformed the cumulative probabilities of the design matrices back to parameter values and simulated model output. Hence, we performed a global uncertainty analysis in a subspace of the entire parameters space that covered 20% of the parameter range of each parameter. This procedure sampled larger intervals for more uncertain parameters and avoided many unreasonable parameter combinations that would occur with a global sensitivity analysis across the entire prior space not accounting for parameter correlations.

We checked robustness of the setting by repeating the analysis by sampling $\pm 20\%$ around the reference parameter values to cover 40% of each parameter range.

While the increased C input simulations (section 2.2) used a high decomposition rate of the residue pool, k_R, for demonstrating stock changes after 50 years, the sensitivity analysis and fluctuation analysis used a lower decomposition rate farther away from the edge of the parameter's prior distribution (Table A1) and simulated increased inputs from year 0 to 100. This helped to avoid severely truncated intervals of sampled parameter space around the decomposition rate.

For each model run, we computed a) the steady state SOM stocks and b) the change in SOM stocks after 100 years of increased C input. The computed sensitivity indexes tell about the proportion of variance in these outputs due to variation in input parameters either by the single effect of a given parameter (first order index) or the combined effect with interaction with other parameters (total sensitivity index) (Saltelli et al., 2008; Sobol, 1990).

Sesam was recoded using the Julia programming language (Bezanson et al., 2017) using package ModelingToolkit.jl (Ma et al., 2021) and solved using method Tsit5 (Tsitouras, 2011) implemented in package DifferentialEquations.jl (Rackauckas and Nie, 2017). This allowed faster simulation and the application of global sensitivity analysis.

2.5 Fluctuation nonlinearity experiment

In order to explore the possible bias in long-term predictions due to the enzyme steady state assumption combined with the nonlinearity of its effect on decomposition we simulated strong seasonal fluctuations in litter inputs causing a seasonal fluctuations in elemental limitation and enzyme community allocation.

SESAM incorporates nonlinear functions. Hence, average decomposition computed with fluctuating enzyme levels will give different results as decomposition computed with first averaging enyzme levels. Hence, the difference between explicitly modeled enzyme levels and steady state state enzyme levels has the potential to introduce bias also in the average long-term predictions.

https://doi.org/10.5194/egusphere-2022-359
Preprint. Discussion started: 4 July 2022

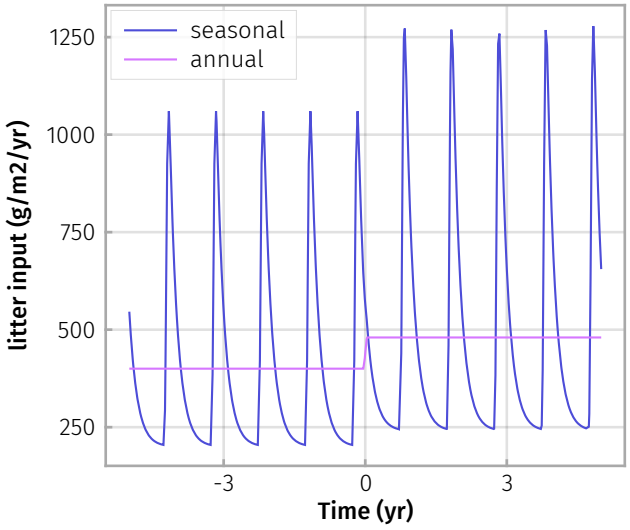

Figure 2. Seasonally fluctuating litter input rate was simulated by assuming 50% of litter input by above-ground litterfall in autumn only. Physical decay of an above-ground litter pool with turnover time of two month then contributed to inputs to the SOM model. At year zero an increase of average annual litter input was prescribed.

In order to investigate the effect of both time-averaging and enzyme steady-state assumption we performed an experiment where we ran both SESAM and a SEAM version, which explicitly tracks enzyme pools but otherwise uses same formulations, with the setting of the increased C input simulation (section 2.2) and seasonally varying litter input. We imposed higher litter input in autumn and lower input during the rest of the year (Fig. 2) and inspected possible bias in the simulation results.

The fluctuating litter scenario displayed stiff properties, hence we used method Vern7 (Verner, 2010) to solve, i.e. simulate the system across time.

3 Results

3.1 Increased C input simulations

The imbalance in stoichiometry with increased C input was compensated by shifting enzyme production towards decomposition of the N-rich residue pool. This led to an increase in litter stocks and a decrease in residue stocks over time (Fig. 3). After input stoichiometry returned to initial conditions, the stocks slowly recovered towards initial state.

Hence, the models simulated microbial N mining, i.e. the behaviour where under increased C input and hence N limitation, N is liberated from SOM. They also simulated the banking mechanism, i.e. the buildup of N rich SOM stocks when N limitation was relieved.

https://doi.org/10.5194/egusphere-2022-359
Preprint. Discussion started: 4 July 2022

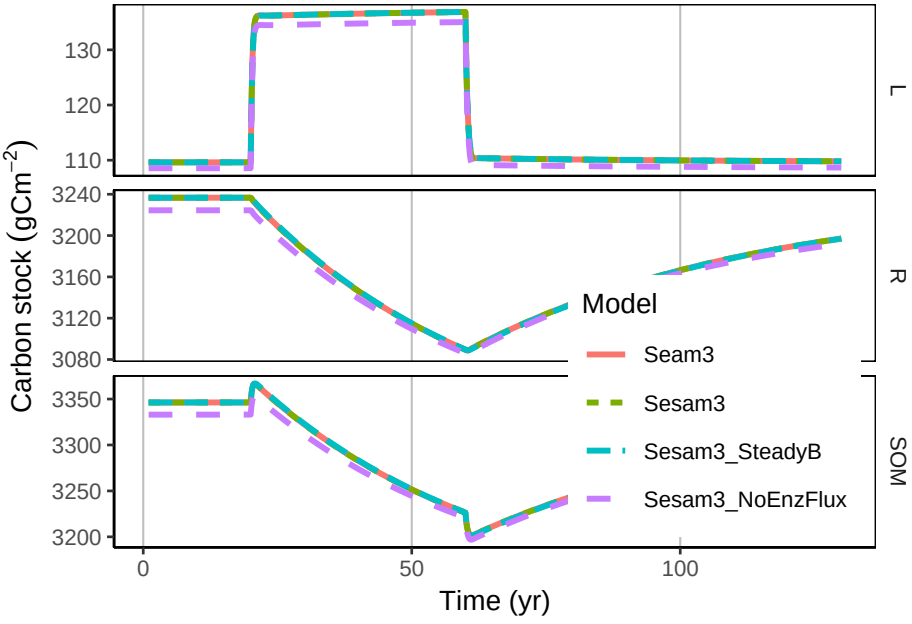

Figure 3. SOM Stocks, the sums of litter, L, and residue, R, develop in the same way with the "Increased C input" simulation with the different model version. All model variants could simulate the liberation of N from organic R stocks with the stoichiometric imbalance with increased C inputs.

At this time scale there were no apparent differences between the enzyme explicit SEAM and the quasi steady state models SESAM and its SteadyB variant. The NoEnzFlux variant lacked a refueling of the DOM pool by the N-rich enzyme turnover, and hence, simulated a residue pool with higher C/N ratio and decomposition slightly shifted towards to residue pool already in initial steady state. However, the variant predicted the same pattern across time.

3.2 Substrate Pulse simulations

CUE varied dynamically in the substrate pulse simulations (Fig. 4). During initial stages there was not enough N in the substrate leading to overflow respiration and low CUE. Lowest CUE was found with highest initial substrate C:N ratios. The subsequent accumulation of microbial residues provided a source of N, which helped increasing the CUE again.

The differences in CUE across time and across initial litter C:N ratios was damped with adaptable enzyme allocation compared to fixed enzyme allocation.

3.3 Sensitivity analysis

SOM stocks and their transient changes in the increased C input simulation were only sensitive to 5 out of 14 model parameters (Fig. 5). As expected, the total stocks in steady state were most sensitive to the potential decomposition rate, k_R , of the

https://doi.org/10.5194/egusphere-2022-359
Preprint. Discussion started: 4 July 2022

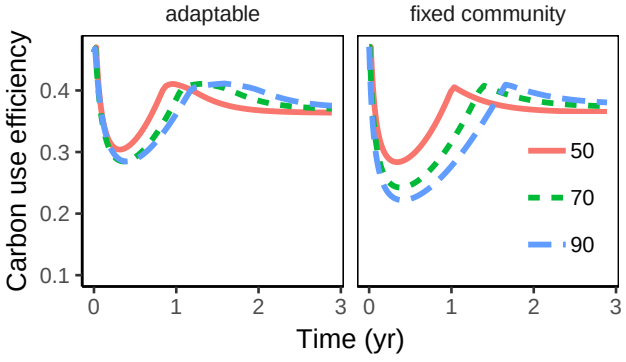

Figure 4. Variation of Carbon use efficiency (CUE) over time with the substrate pulse simulation is more conserved with community adaptable enzyme allocation than with fixed allocation, both across time (x-axis) and across initial substrate C/N ratio (line color and line type).

residue pool, which is the largest SOM pool. In addition, they were sensitive to parameters of microbial turnover, τ and ϵ_{tvr}, and turnover of enzymes, k_{mN}. Transient changes of SOM stocks were also sensitive to microbial turnover, but not to decomposition rate. Rather they were sensitive to stoichiometric parameters, specifically the C/N ratio of microbial biomass, β_{NB}, and the intrinsic CUE, ϵ.

When repeating the sensitivity analysis on a subspace that included 40% rather than 20% of each parameters range, the results were influenced by extreme values due to unusual parameter combinations. We observed similar total effects of SOM stocks but first order effects were slightly smaller. SOM stock changes now were additionally sensitive to decomposition rate, k_R, and the sensitivity to C/N ratio of microbial biomass, β_{NB} was less strong (appendix Fig. C1).

3.4 Fluctuation analysis

Simulation results differed only marginally between steady state enzymes (SESAM) and explicit representation of enzyme level (SEAM) in the fluctuating litter input simulations (Fig 6, sesam_annual overplotting seam_annual). This resulted from steady state enzyme being close to the explicit enzyme levels (appendix D). Hence, the enzyme steady state assumptions did not introduce bias in predictions.

Fluxes based on averaging litter inputs also roughly matched the average of the fluxes based on fluctuating litter inputs at steady state (Fig. 6 before increase of C input at time $t < 0$). Hence, also averaging litter inputs did not introduce bias at steady state.

Largest simulated differences due to averaging litter input were observed in transient changes of the fast pools, e.g. the inorganic N pool and associated leaching (Fig. 6 after increase of C input at time $t > 0$). This is expected because immediate transient changes depend on the timing of litter inputs within the year.

https://doi.org/10.5194/egusphere-2022-359
Preprint. Discussion started: 4 July 2022

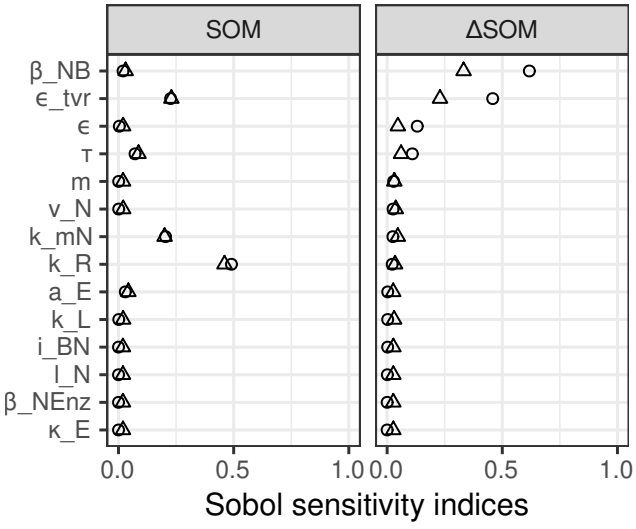

Figure 5. Simulated stock change with increased C litter input (ΔSOM), was most sensitive to C/N ratio of microbial biomass (β_{NB}), while initial steady state stocks (SOM) was most sensitive to turnover rate of residue pool (k_R). Both were sensitive to parameters of microbial turnover. While effects on stocks were mostly direct (indicated by first order effects (triangles) were similar to total effect (circles)), the stock changes were mostly sensitive to interactions of parameters.

4 Discussion

4.1 Decadal-scale SOM cycling

Soil organic matter (SOM) science has experienced a paradigm shift from understanding persistence of OM soils formerly on chemical OM properties towards understanding persistence as an interactive effect of environmental conditions (Schmidt et al., 2011). At the heart of the interactions are soil microbial processes, and hence, these processes need to be represented in models of SOM dynamics. Indeed, microbial models have shown to be able to better represent global patters of SOM stocks (Wieder et al., 2013) However, details of representing these microbial processes lead to qualitatively different predictions. Furthermore, hard to get observations as required to constrain its parameters (Marschmann et al., 2019).

Many of these processes work on small spatial and temporal scale. In this work we pursue the hypothesis that at longer decadal-term scale, stoichiometry provides one of the most important constraints (Buchkowski et al., 2019), and that at this scale, we can abstract from many detailed processes but still keep the mean effects. We apply the quasi steady state (QSS) assumption that separates processes at different time scales (Wutzler and Reichstein, 2013).

Averaging inputs together with nonlinear functions can cause bias (Chakrawal et al., 2020; Graham et al., 2019). And the timing of litter inputs can be important (Luu et al., 2022; Zhou et al., 2021). The presented SESAM model assumes enzyme levels in steady state (section 2.1.2). Hence, SESAM was expected to not precisely reproduce seasonal dynamics with

https://doi.org/10.5194/egusphere-2022-359
Preprint. Discussion started: 4 July 2022

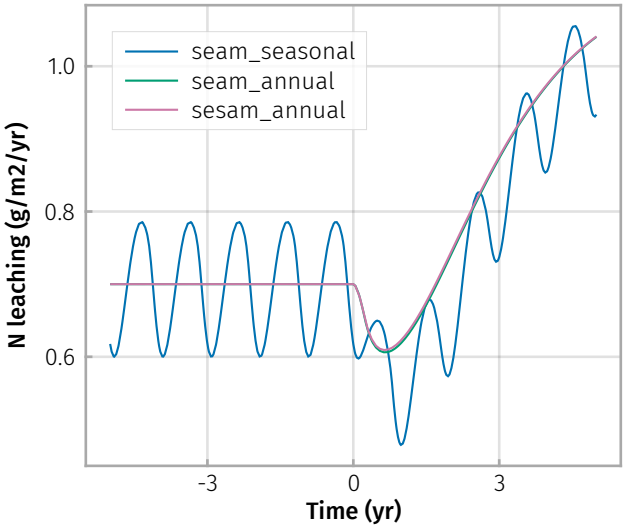

Figure 6. Small differences in transient N-leaching between simulation scenarios of seasonally fluctuating litter input (wiggling curves) and annually averaged litter inputs (smooth curves) were caused by different timing of litter input between the scenarios after the prescribed increase of average annual inputs at year zero. Abstraction of enzyme steady states (sesam) did not cause additional differences between the litter scenarios, as seen by overplotting.

litter inputs due to nonlinear effects of enzymes on decomposition. SESAM does not model microbial strategies to cope with varying litter stoichiometry such as internal reserves (Manzoni et al., 2021) nor energetic trade-offs (Dufour et al., 2021) and neglects smoothing dynamics that occurs when explicitly modeling DOM and enzyme pools. Hence it may predict overflow respiration or excess N mineralization due to short term fluctuations of stoichiometric imbalance in uptake of DOM. Therefore, we recommend driving SESAM with annually averaged model inputs.

The mostly concave functions of decomposition according to Michaelis-Menten kinetics yield a lower flux of the average input compared to the average of the fluxes on varying input. Hence, we expected slightly higher decomposition rates and lower stocks with the average litter input scenario. The fluctuation analysis revealed, fortunately, that due to inherent dynamics of community pools, there was no apparent bias due to the enzyme steady state assumption, and only small transient deviations in averaged predictions by driving SESAM with annually averaged litter inputs in the compared to supplying seasonally fluctuating litter inputs (Fig 6). This shows that SESAM may be applicable also at shorter time scales under certaint conditions, although the model has been primarily designed to predict effect of decadal-term changes considering average model inputs.

4.2 Simulate patterns emerging from microbial processes

Competition between microbial groups and adaptation of the microbial community is one of those detailed processes that have been shown to exert strong control on decadal-term SOM dynamics. SESAM represents such competition by modeling

https://doi.org/10.5194/egusphere-2022-359
Preprint. Discussion started: 4 July 2022

adaptation of community traits, specifically the allocation of enzyme production. We performed simulation experiments to see whether the model can predict similar patterns as more detailed models. The "Substrate pulse simulations" (Fig. 4) reproduced the pattern shown by Kaiser et al. (2014) of more conserved CUE with microbial adaptation. Avoiding the low CUE with litter pulses by shifting the community to grow more on the N-rich substrates helps sequestering more C to the soil pools instead of respiring it to the atmosphere after those pulses. The "Increase C input simulations" (Fig. 3) reproduced the pattern shown by Perveen et al. (2014) of liberating N from SOM stocks during conditions of imbalanced higher C inputs. Making this N available for plants helps them to avoid or delay progressive N limitation (Averill et al., 2015).

Whether increased C inputs leads to decrease of SOM due to priming or to increase of SUM due to larger input of microbial turnover to SOM is one of the open question discussion in soil science. It probably depends on the combination of other constraints such as nutrient availability (Hicks et al., 2021; Vain et al., 2021; Feng and Zhu, 2021). Studying and discussing how these pathways can be modeled and clarified using SESAM warrants a dedicated manuscript. SESAM predicts a change in proportion of different SOM pools in response to shifting nutrient limitations. While the relative changes in SOM pools are so small that are very hard to directly measure, changes can potentially be detected by a changing C/N ratio of the total SOM (vandenEnden et al., 2021; Melillo, 2019).

4.3 Model complexity and identifiability

Optimal detail or complexity of models depends on the purpose of the model and on the available data to constrain the models (Jakeman et al., 2006). Microbial processes are strongly determined by pore-scale environment (Pot et al., 2021; Kaiser et al., 2014) and available data is mostly from laboratory and from short time scales. Larger scale compilations are available for stoichiometry of litter, microbial biomass and enzyme activities (Xu et al., 2013; Zechmeister-Boltenstern et al., 2015) but scarce for growth and turnover rates (Spohn et al., 2016), element use efficiencies (Manzoni et al., 2018), and very rare for different groups of microbes. Hence, microbial parameters need to be constrained by inverting models to larger scale observations.

There are many attempts to directly implement microbial processes into global models with introducing many free parameters (Campbell and Paustian, 2015). For example the ORCHIMIC (Huang et al., 2018) explicitly models several microbial functional types and active and dormant fractions. It introduces $n_{Group} * 11$ microbial parameters. More parameters raise the problem of model identifiability in model inversions. The model may fit the observations for the wrong reasons and predictions then likely fail for conditions different from that of the calibration.

SESAM aims at reducing model complexity. There are in total 14 model parameters and long-term SOM stock changes were sensitive to only a few of them. This is a more tractable number of parameters for model inversions, although there will be more parameters for temperature and moisture dependencies and transport when integrated into larger models. Because SESAM targets decadal-term scale, also decadal term drivers and observations should be used in SESAM model-data integration studies. Currently, the free air enrichment time series are running about 20 years are getting long enough to calibrate and test models at decadal time scale.

https://doi.org/10.5194/egusphere-2022-359
Preprint. Discussion started: 4 July 2022

4.4 Sensitivity of predictions to microbial properties

C/N ratio of microbial biomass, β_{BN} was the most sensitive parameter for SOM changes (Fig.5). Hence, the assumption that it can be fixed because its range it rather constrained has to be revisited. We think of ways how let it change together with other microbial properties of enzyme allocation.

The turnover rate of microbial biomass, τ was also among the most sensitive parameters. One reason is that it contributes an important source for inorganic N when Microbes are N limited (Joly et al., 2020; Clarholm, 1985). Without predation of microbes and associated mineralization, N would be largely locked in the organic loop.

In SESAM microbial turnover it is currently modeled first order to microbial biomass and predation as a fixed factor of this turnover. A part of the turnover feeds to the DOM pool and a part adds to the residue pool. Developments of SESAM focus on refining those processes in several ways. Predation rate is smaller at low microbial biomass when predators have to move farther between encountering microbes. Further, the stoichiometry of the parts feeding to DOM and the residue pool will be different, because there is different cell material in lysed cell and cell walls. Differences in stoichiometry of microbial decay becoming DOM and decay becoming residue will have a large impact on modeled SOM stocks (Yu et al., 2020a).

4.5 Outlook

Another avenue forward is studying the effect of stoichiometric constraints by other elements than C and N. The next step is to include phosphorus (P) constraints. A first implementation in the JSM model (Yu et al., 2020b) revealed several challenges. In a process called biomineralization, oxidative enzymes can liberate P from OM without making other elements available in stoichiometric proportion. Moreover, enzyme levels and revenue are also more strongly affected by plant root enzyme production, and additionally, the revenue computation already has been adapted to account for the low P cost of enzymes production under P limitation.

Furthermore, the SESAM scheme needs to be tested in context of more comprehensive soil model that includes temperature and moisture modifiers, transport, and protection by the mineral matrix.

5 Conclusions

The application of the quasi-steady-state assumption for extracellular enzyme pools simplified a model of microbial adaptation to substrate stoichiometry. The simplified SESAM model could reproduce important effects of microbial stoichiometry on SOM dynamics at decadal time scale, specifically, the priming effect, microbial N mining, the SOM banking mechanism, and conserving CUE. This development is an important step towards more parsimonious representation of soil microbial effects in global land surface models.

https://doi.org/10.5194/egusphere-2022-359
Preprint. Discussion started: 4 July 2022

5.1 Code and data availability

SESAM (v3.0) is available coded in R at https://github.com/bgctw/sesam (doi: 10.5281/zenodo.6758806) and coded in Julia at https://github.com/bgctw/Sesam.jl (doi: 10.5281/zenodo.6758868). R source code is released using the GPL-2 licence, because it uses other GPL libraries. Julia code is released using the more permissive MIT License.

The model version comparison code of this study is part of the R repository in file develop/19GMD_paper/CompareModels.Rmd. The sensitivity analysis code of this study is part of the Julia repository at inst/22paper_upscaling/sensitivity_Face.jl and the fluctuation analysis in inst/22paper_upscaling/fluctuation_analysis.jl.

Author contributions. TW developed the model, and led the writing of the manuscript. LY implemented SESAM into a larger land model, which initiated several reformulations of model aspects. All authors contributed to discussion and writing of the manuscript.

Competing interests. No competing interests are present

Acknowledgements. WE thank Bernhard Ahrens and Markus Reichstein for fruitful discussion. We thank the Max Planck society for funding. LY is supported by the Swedish government-funded Strategic Research Area Biodiversity and Ecosystems in a Changing Climate, BECC

https://doi.org/10.5194/egusphere-2022-359
Preprint. Discussion started: 4 July 2022

References

Allison, S. D.: Modeling adaptation of carbon use efficiency in microbial communities, Frontiers in Microbiology, 5, https://doi.org/10.3389/fmicb.2014.00571, 2014.

Averill, C., Rousk, J., and Hawkes, C.: Microbial-mediated redistribution of ecosystem nitrogen cycling can delay progressive nitrogen limitation, Biogeochemistry, 126, 11–23, https://doi.org/10.1007/s10533-015-0160-x, 2015.

Bezanson, J., Edelman, A., Karpinski, S., and Shah, V. B.: Julia: A fresh approach to numerical computing, SIAM review, 59, 65–98, 2017.

Bradford, M. A., Wieder, W. R., Bonan, G. B., Fierer, N., Raymond, P. A., and Crowther, T. W.: Managing uncertainty in soil carbon feedbacks to climate change, Nature Climate Change, 6, 751–758, https://doi.org/10.1038/nclimate3071, 2016.

Buchkowski, R. W., Shaw, A. N., Sihi, D., Smith, G. R., and Keiser, A. D.: Constraining Carbon and Nutrient Flows in Soil With Ecological Stoichiometry, Frontiers in Ecology and Evolution, 7, https://doi.org/10.3389/fevo.2019.00382, 2019.

Campbell, E. E. and Paustian, K.: Current developments in soil organic matter modeling and the expansion of model applications: a review, Environmental Research Letters, 10, 123 004, https://doi.org/10.1088/1748-9326/10/12/123004, 2015.

Chakrawal, A., Herrmann, A. M., Koestel, J., Jarsjö, J., Nunan, N., Kätterer, T., and Manzoni, S.: Dynamic upscaling of decomposition kinetics for carbon cycling models, Geoscientific Model Development, 13, 1399–1429, https://doi.org/10.5194/gmd-13-1399-2020, 2020.

Clarholm, M.: Interactions of bacteria, protozoa and plants leading to mineralization of soil nitrogen, Soil Biology and Biochemistry, 17, 181–187, https://doi.org/10.1016/0038-0717(85)90113-0, 1985.

Cleveland, C. C. and Liptzin, D.: C:N:P stoichiometry in soil: is there a Redfield ratio for the microbial biomass?, Biogeochemistry, 85, 235–252, https://doi.org/10.1007/s10533-007-9132-0, 2007.

Dufour, L., Herrmann, A., Leloup, J., Przybylski, C., Foti, L., Abbadie, L., and Nunan, N.: Energetic return on investment determines overall soil microbial activity., Research Square, https://doi.org/10.21203/rs.3.rs-388050/v1, 2021.

Fatichi, S., Manzoni, S., Or, D., and Paschalis, A.: A Mechanistic Model of Microbially Mediated Soil Biogeochemical Processes: A Reality Check, Global Biogeochemical Cycles, 33, 620–648, https://doi.org/10.1029/2018gb006077, 2019.

Feng, J. and Zhu, B.: Global patterns and associated drivers of priming effect in response to nutrient addition, Soil Biology and Biochemistry, 153, 108 118, https://doi.org/10.1016/j.soilbio.2020.108118, 2021.

Graham, L. J., Spake, R., Gillings, S., Watts, K., and Eigenbrod, F.: Incorporating fine-scale environmental heterogeneity into broad-extent models, Methods in Ecology and Evolution, 10, 767–778, https://doi.org/10.1111/2041-210x.13177, 2019.

Guenet, B., Moyano, F. E., Peylin, P., Ciais, P., and Janssens, I. A.: Towards a representation of priming on soil carbon decomposition in the global land biosphere model ORCHIDEE (version 1.9.5.2), Geoscientific Model Development, 9, 841–855, https://doi.org/10.5194/gmd-9-841-2016, 2016.

Hagerty, S. B., Allison, S. D., and Schimel, J. P.: Evaluating soil microbial carbon use efficiency explicitly as a function of cellular processes: implications for measurements and models, Biogeochemistry, 140, 269–283, https://doi.org/10.1007/s10533-018-0489-z, 2018.

Hicks, L. C., Lajtha, K., and Rousk, J.: Nutrient limitation may induce microbial mining for resources from persistent soil organic matter, Ecology, 102, https://doi.org/10.1002/ecy.3328, 2021.

Huang, Y., Guenet, B., Ciais, P., Janssens, I. A., Soong, J. L., Wang, Y., Goll, D., Blagodatskaya, E., and Huang, Y.: ORCHIMIC (v1.0), a microbe-mediated model for soil organic matter decomposition, Geoscientific Model Development, 11, 2111–2138, https://doi.org/10.5194/gmd-11-2111-2018, 2018.

https://doi.org/10.5194/egusphere-2022-359
Preprint. Discussion started: 4 July 2022

Jakeman, A. J., Letcher, R. A., and Norton, J. P.: Ten iterative steps in development and evaluation of environmental models, Environmental Modelling & Software, 21, 602–614, 2006.

Janssens, I. A., Dieleman, W., Luyssaert, S., Subke, J.-A., Reichstein, M., Ceulemans, R., Ciais, P., Dolman, A. J., Grace, J., Matteucci, G., and et al.: Reduction of forest soil respiration in response to nitrogen deposition, Nature Geoscience, 3, 315–322, 2010.

Joly, F.-X., Coq, S., Coulis, M., David, J.-F., Hättenschwiler, S., Mueller, C. W., Prater, I., and Subke, J.-A.: Detritivore conversion of litter into faeces accelerates organic matter turnover, Communications Biology, 3, https://doi.org/10.1038/s42003-020-01392-4, 2020.

Kaiser, C., Franklin, O., Dieckmann, U., and Richter, A.: Microbial community dynamics alleviate stoichiometric constraints during litter decay, Ecology Letters, 17, 680–690, https://doi.org/10.1111/ele.12269, 2014.

Kuzyakov, Y.: Priming effects: Interactions between living and dead organic matter, Soil Biology and Biochemistry, In Press, Uncorrected Proof, –, https://doi.org/DOI: 10.1016/j.soilbio.2010.04.003, 2010.

Li, T., Wang, R., Cai, J., Meng, Y., Wang, Z., Feng, X., Liu, H., Turco, R. F., and Jiang, Y.: Enhanced carbon acquisition and use efficiency alleviate microbial carbon relative to nitrogen limitation under soil acidification, Ecological Processes, 10, https://doi.org/10.1186/s13717-021-00309-1, 2021.

Liu, W., Qiao, C., Yang, S., Bai, W., and Liu, L.: Microbial carbon use efficiency and priming effect regulate soil carbon storage under nitrogen deposition by slowing soil organic matter decomposition, Geoderma, 332, 37–44, https://doi.org/10.1016/j.geoderma.2018.07.008, 2018.

Luu, A. T., Hoang, N. T., Dinh, V. M., Bui, M. H., Grandy, S., and Hoang, D. T. T.: Effects of carbon input quality and timing on soil microbe mediated processes, Geoderma, 409, 115 605, https://doi.org/10.1016/j.geoderma.2021.115605, 2022.

Ma, Y., Gowda, S., Anantharaman, R., Laughman, C., Shah, V., and Rackauckas, C.: ModelingToolkit: A Composable Graph Transformation System For Equation-Based Modeling, 2021.

Manzoni, S., Porporato, A., and Schimel, J. P.: Soil heterogeneity in lumped mineralization-immobilization models, Soil Biology & Biochemistry, 40, 1137–1148, https://doi.org/10.1016/j.soilbio.2007.12.006, 2008.

Manzoni, S., Čapek, P., Porada, P., Thurner, M., Winterdahl, M., Beer, C., Brüchert, V., Frouz, J., Herrmann, A. M., Lindahl, B. D., Lyon, S. W., Šantrůčková, H., Vico, G., and Way, D.: Reviews and syntheses: Carbon use efficiency from organisms to ecosystems – definitions, theories, and empirical evidence, Biogeosciences, 15, 5929–5949, https://doi.org/10.5194/bg-15-5929-2018, 2018.

Manzoni, S., Ding, Y., Warren, C., Banfield, C. C., Dippold, M. A., and Mason-Jones, K.: Intracellular storage reduces stoichiometric imbalances in soil microbial biomass–A theoretical exploration, Frontiers in Ecology and Evolution, p. 663, https://doi.org/10.1038/s41396-021-01110-w, 2021.

Marschmann, G. L., Pagel, H., Kügler, P., and Streck, T.: Equifinality, sloppiness, and emergent structures of mechanistic soil biogeochemical models, Environmental Modelling & Software, 122, 104 518, https://doi.org/10.1016/j.envsoft.2019.104518, 2019.

Melillo, J.: Changes in Soil Carbon Dynamics in Response to Long-Term Soil Warming - Integration Across Scales from Cells to Ecosystems, Tech. rep., DOE's Office of Science (BER), https://doi.org/10.2172/1502957, 2019.

Moorhead, D. L., Lashermes, G., and Sinsabaugh, R. L.: A theoretical model of C-and N-acquiring exoenzyme activities, which balances microbial demands during decomposition, Soil Biology and Biochemistry, 53, 133–141, https://doi.org/10.1016/j.soilbio.2012.05.011, 2012.

Mooshammer, M., Wanek, W., Hämmerle, I., Fuchslueger, L., Hofhansl, F., Knoltsch, A., Schnecker, J., Takriti, M., Watzka, M., Wild, B., and et al.: Adjustment of microbial nitrogen use efficiency to carbon:nitrogen imbalances regulates soil nitrogen cycling, Nature Communications, 5, 2014a.

https://doi.org/10.5194/egusphere-2022-359
Preprint. Discussion started: 4 July 2022

Mooshammer, M., Wanek, W., Zechmeister-Boltenstern, S., and Richter, A.: Stoichiometric imbalances between terrestrial decomposer communities and their resources: mechanisms and implications of microbial adaptations to their resources, Frontiers in Microbiology, 5, https://doi.org/10.3389/fmicb.2014.00022, 2014b.

Perveen, N., Barot, S., Alvarez, G., Klumpp, K., Martin, R., Rapaport, A., Herfurth, D., Louault, F., and Fontaine, S.: Priming effect and microbial diversity in ecosystem functioning and response to global change: a modeling approach using the SYMPHONY model, Global Change Biology, 20, 1174 – 1190, https://doi.org/10.1111/gcb.12493, 2014.

Pot, V., Portell, X., Otten, W., Garnier, P., Monga, O., and Baveye, P. C.: Accounting for soil architecture and microbial dynamics in microscale models: Current practices in soil science and the path ahead, European Journal of Soil Science, https://doi.org/10.1111/ejss.13142, 2021.

R Core Team: R: A Language and Environment for Statistical Computing, R Foundation for Statistical Computing, Vienna, Austria, 2021.

Rackauckas, C. and Nie, Q.: Differentialequations.jl - a performant and feature-rich ecosystem for solving differential equations in julia, Journal of Open Research Software, 5, 15, 2017.

Rastetter, E. B.: Modeling coupled biogeochemical cycles, Frontiers in Ecology and the Environment, 9, 68 – 73, https://doi.org/10.1890/090223, 2011.

Saltelli, A., Ratto, M., Andres, T., Campolongo, F., Cariboni, J., Gatelli, D., Saisana, M., and Tarantola, S.: Global Sensitivity Analysis. The Primer, John Wiley & Sons, 1 edn., 2008.

Schimel, J. P. and Weintraub, M. N.: The implications of exoenzyme activity on microbial carbon and nitrogen limitation in soil: a theoretical model, Soil Biology and Biochemistry, 35, 549–563, 2003.

Schmidt, M. W. I., Torn, M. S., Abiven, S., Dittmar, T., Guggenberger, G., Janssens, I. A., Kleber, M., Kogel-Knabner, I., Lehmann, J., Manning, D. A. C., Nannipieri, P., Rasse, D. P., Weiner, S., and Trumbore, S. E.: Persistence of soil organic matter as an ecosystem property, Nature, 478, 49–56, https://doi.org/10.1038/nature10386, 2011.

Sinsabaugh, R. L., Manzoni, S., Moorhead, D. L., and Richter, A.: Carbon use efficiency of microbial communities: stoichiometry, methodology and modelling, Ecology Letters, 16, 930–939, https://doi.org/10.1111/ele.12113, 2013.

Sobol, I. M.: On sensitivity estimation for nonlinear mathematical models, Matem. Mod., 2, 112–118, 1990.

Soetaert, K., Petzoldt, T., and Setzer, R.: R Package deSolve, Writing Code in Compiled Languages, R package vignette, URL http://CRAN. R-project. org/package= deSolve, 2009.

Spohn, M., Klaus, K., Wanek, W., and Richter, A.: Microbial carbon use efficiency and biomass turnover times depending on soil depth â€“ Implications for carbon cycling, Soil Biology and Biochemistry, 96, 74–81, https://doi.org/10.1016/j.soilbio.2016.01.016, 2016.

Sterner, R. W. and Elser, J. J.: Ecological stoichiometry: the biology of elements from molecules to the biosphere, Princeton University Press, 2002.

Tang, J. and Riley, W. J.: Weaker soil carbon–climate feedbacks resulting from microbial and abiotic interactions, Nature Climate Change, 5, 56–60, https://doi.org/10.1038/nclimate2438, 2014.

Tang, J. and Riley, W. J.: Competitor and substrate sizes and diffusion together define enzymatic depolymerization and microbial substrate uptake rates, Soil Biology and Biochemistry, 139, 107 624, https://doi.org/10.1016/j.soilbio.2019.107624, 2019.

Thornton, P. E., Lamarque, J.-F., Rosenbloom, N. A., and Mahowald, N. M.: Influence of carbon-nitrogen cycle coupling on land model response to CO 2 fertilization and climate variability, Global Biogeochemical Cycles, 21, https://doi.org/10.1029/2006gb002868, 2007.

Todd-Brown, K. E. O., Hopkins, F. M., Kivlin, S. N., Talbot, J. M., and Allison, S. D.: A framework for representing microbial decomposition in coupled climate models, Biogeochemistry, 109, 19–33, https://doi.org/10.1007/s10533-011-9635-6, 2012.

https://doi.org/10.5194/egusphere-2022-359
Preprint. Discussion started: 4 July 2022

Tsitouras, C.: Runge-Kutta pairs of order 5 (4) satisfying only the first column simplifying assumption, Computers & Mathematics with Applications, 62, 770–775, 2011.

Vain, A.-C., Rakotondrazafy, N., Razanamalala, K., Trap, J., Marsden, C., Blanchart, E., and Bernard, L.: The fate of primed soil carbon between biomass immobilization and respiration is controlled by nutrient availability, European Journal of Soil Biology, 105, 103 332, https://doi.org/10.1016/j.ejsobi.2021.103332, 2021.

vandenEnden, L., Anthony, M. A., Frey, S. D., and Simpson, M. J.: Biogeochemical evolution of soil organic matter composition after a decade of warming and nitrogen addition, Biogeochemistry, https://doi.org/10.1007/s10533-021-00837-0, 2021.

Verner, J. H.: Numerically optimal Runge-Kutta pairs with interpolants, Numerical Algorithms, 53, 383–396, 2010.

Wieder, W. R., Bonan, G. B., and Allison, S. D.: Global soil carbon projections are improved by modelling microbial processes, Nature Climate Change, https://doi.org/10.1038/nclimate1951, 2013.

Wutzler, T. and Reichstein, M.: Priming and substrate quality interactions in soil organic matter models, Biogeosciences, 10, 2089–2103, https://doi.org/10.5194/bg-10-2089-2013, 2013.

Wutzler, T., Zaehle, S., Schrumpf, M., Ahrens, B., and Reichstein, M.: Adaptation of microbial resource allocation affects modelled long term soil organic matter and nutrient cycling, Soil Biology and Biochemistry, 115, 322–336, https://doi.org/10.1016/j.soilbio.2017.08.031, 2017.

Xu, X., Thornton, P. E., and Post, W. M.: A global analysis of soil microbial biomass carbon, nitrogen and phosphorus in terrestrial ecosystems, Global Ecology and Biogeography, 22, 737–749, https://doi.org/10.1111/geb.12029, 2013.

Xu, X., Schimel, J. P., Thornton, P. E., Song, X., Yuan, F., and Goswami, S.: Substrate and environmental controls on microbial assimilation of soil organic carbon: a framework for Earth system models, Ecology letters, 17, 547–555, https://doi.org/10.1111/ele.12254, 2014.

Yu, L., Ahrens, B., Wutzler, T., Schrumpf, M., and Zaehle, S.: Jena Soil Model (JSM v1.0 revision 1934): a microbial soil organic carbon model integrated with nitrogen and phosphorus processes, Geoscientific Model Development, 13, 783–803, https://doi.org/10.5194/gmd-13-783-2020, 2020a.

Yu, L., Ahrens, B., Wutzler, T., Zaehle, S., and Schrumpf, M.: Modeling Soil Responses to Nitrogen and Phosphorus Fertilization Along a Soil Phosphorus Stock Gradient, Frontiers in Forests and Global Change, 3, https://doi.org/10.3389/ffgc.2020.543112, 2020b.

Zaehle, S. and Dalmonech, D.: Carbon-nitrogen interactions on land at global scales: current understanding in modelling climate biosphere feedbacks, Current Opinion in Environmental Sustainability, 3, 311–320, https://doi.org/10.1016/j.cosust.2011.08.008, 2011.

Zechmeister-Boltenstern, S., Keiblinger, K. M., Mooshammer, M., Penuelas, J., Richter, A., Sardans, J., and Wanek, W.: The application of ecological stoichiometry to plant - microbial - soil organic matter transformations, Ecological Monographs, 85, 133–155, https://doi.org/10.1890/14-0777.1, 2015.

Zhou, J., Wen, Y., Shi, L., Marshall, M. R., Kuzyakov, Y., Blagodatskaya, E., and Zang, H.: Strong priming of soil organic matter induced by frequent input of labile carbon, Soil Biology and Biochemistry, 152, 108 069, https://doi.org/10.1016/j.soilbio.2020.108069, 2021.

Appendix A: SESAM equations

For an overview of symbol definitions see tables 1, A1, and A2.

https://doi.org/10.5194/egusphere-2022-359
Preprint. Discussion started: 4 July 2022

Table A1. Model parameters and distributions used in the sensitivity analysis.

Symbol	Definition	Value	Unit	Prior distribution	q025	mode	q975
$\beta_{N\,B}$	C/N ratio of microbial biomass	11	$\mathrm{g\,g^{-1}}$	LogNormal(2.08,0.35)	4.0	8.0	16.0
$\beta_{N\,Enz}$	C/N ratio of extracellular enzymes	3.1	$\mathrm{g\,g^{-1}}$	LogNormal(1.1,0.079)	2.6	3.0	3.5
k_R	maximum decomposition rate of R	0.0025	$\mathrm{yr^{-1}}$	LogNormal(-4.61,1.2)	0.001	0.01	0.1
k_L	maximum decomposition rate of L	1.0	$\mathrm{yr^{-1}}$	LogNormal(-0.41,0.77)	0.15	0.67	3.0
κ_E	fraction enzyme tvr. entering DOM instead R	0.8	(-)	LogNormal(-0.36,0.13)	0.54	0.7	0.9
a_E	enzyme production per microbial biomass	0.365	$\mathrm{yr^{-1}}$	LogNormal(-1.01,0.82)	0.073	0.36	1.8
k_{mN}	product of enzyme half saturation constant and enzyme turnover	3.0	$\mathrm{g\,m^{-2}}$	LogNormal(1.1,2.2)	0.037	3.0	240.0
τ	microbial biomass turnover rate	6.1	$\mathrm{yr^{-1}}$	LogNormal(1.81,1.3)	0.51	6.1	73.0
m	specific rate of maintenance respiration	1.8	$\mathrm{yr^{-1}}$	LogNormal(0.6,0.71)	0.46	1.8	7.3
ϵ	anabolic microbial C substrate efficiency	0.5	(-)	LogitNormal(0.0,0.43)	0.3	0.5	0.7
ϵ_{tvr}	microbial turnover that is not mineralized	0.45	(-)	LogitNormal(-0.85,1.6)	0.02	0.3	0.9
ν_N	aggregated microbial organic N use efficiency	0.9	(-)	LogNormal(-0.11,0.049)	0.82	0.9	0.99
i_{BN}	maximum microbial uptake rate of inorganic N	0.4	$\mathrm{yr^{-1}}$	LogNormal(-0.92,1.2)	0.04	0.4	4.0
l_N	inorganic N leaching rate	0.96	$\mathrm{yr^{-1}}$	LogNormal(-0.04,0.82)	0.19	0.96	4.8

A1 Carbon dynamics

$$\frac{dB}{dt} = \mathrm{syn}_B - \mathrm{tvr}_B \tag{A1a}$$

$$\frac{dL}{dt} = -\mathrm{dec}_L + \mathrm{i}_L(t) \tag{A1b}$$

$$\frac{dR}{dt} = -\mathrm{dec}_R + \epsilon_{\mathrm{tvr}}\,\mathrm{tvr}_B + (1-\kappa_E)\,\mathrm{syn}_{\mathrm{Enz}}, \tag{A1c}$$

where ϵ_{tvr} is the fraction of microbial turnover C that is respired by predators, i_L is the litter C input to the system, and κ_E is the fraction of enzyme turnover that is transferred to the DOM instead of the R pool. Details of the specific fluxes are given below.

https://doi.org/10.5194/egusphere-2022-359
Preprint. Discussion started: 4 July 2022

Table A2. Further symbols of quantities derived within the system

Symbol	Definition	Unit
syn_B	C for microbial biomass synthesis	$\mathrm{g\,m^{-2}yr^{-1}}$
$\mathrm{syn}_{\mathrm{Enz}}$	C synthesis of enzymes	$\mathrm{g\,m^{-2}yr^{-1}}$
tvr_B	microbial biomass turnover C	$\mathrm{g\,m^{-2}yr^{-1}}$
dec_S	C in depolymerization of resource $S \in \{L, R\}$	$\mathrm{g\,m^{-2}yr^{-1}}$
u_C, u_N	microbial uptake of C and N	$\mathrm{g\,m^{-2}yr^{-1}}$
Φ_{uE}, Φ_{EB}, $\Phi_{\mathrm{tvr}\,E}$, Φ_E	mineralization of element $E \in \{N\}$ with microbial DOM uptake, stoichiometric imbalance, turnover, and total $\Phi = \Phi_u + \Phi_B + \Phi_{\mathrm{tvr}}$ (Fig. A1)	$\mathrm{g\,m^{-2}yr^{-1}}$

Total enzyme production $\mathrm{syn}_{\mathrm{Enz}}$, maintenance respiration r_M, and microbial turnover tvr_B are modeled as a first-order kinetics of biomass:

$$\mathrm{syn}_{\mathrm{Enz}} = a_E B \tag{A2a}$$

$$\mathrm{r}_M = mB \tag{A2b}$$

$$\mathrm{tvr}_B = \tau B \tag{A2c}$$

With assuming enzyme production and turnover to be in quasi steady state and reverse Michaelis-Menten kinetics for substrate decomposition (Schimel and Weintraub, 2003; Tang and Riley, 2019), substrate depolymerisation is:

$$\mathrm{dec}_{S,Pot} = k_S S \tag{A3a}$$

$$\mathrm{dec}_S = \mathrm{dec}_{S,Pot} \frac{\alpha_S\ \mathrm{syn}_{\mathrm{Enz}}}{k_{mN} + \alpha_S\ \mathrm{syn}_{\mathrm{Enz}}} \tag{A3b}$$

where $\mathrm{dec}_{S,Pot}$ is the decomposition flux when enzymes are saturated, $S \in \{L, R\}$ is one of the substrate pools, k_S is the maximum decomposition rate of S, α_S is the proportion of total investment into enzymes that is allocated to S (section A4), and k_{mN} is a lumped parameter of enzyme half-saturation constant and enzyme turnover.

We assume quasi steady state of the DOM pool, and hence, microbial uptake equals the sum of all influxes to the DOM pool (decomposition + part of the enzyme turnover).

$$u_C = \mathrm{dec}_L + \mathrm{dec}_R + \kappa_E\,\mathrm{syn}_{\mathrm{Enz}} \tag{A4}$$

https://doi.org/10.5194/egusphere-2022-359
Preprint. Discussion started: 4 July 2022

With C limitation, C_{synBC}, the carbon available for synthesis of new biomass, equals the C uptake minus the expenses for enzyme synthesis (eq. A2a) and maintenance respiration (eq. A2b). If this balance is positive, then a part is used for growth respiration.

$$C_{\mathrm{synBCt}} = u_C - \mathrm{syn}_{\mathrm{Enz}}/\epsilon - \mathrm{r}_M \tag{A5a}$$

$$C_{\mathrm{synBC}} = \begin{cases} \epsilon C_{\mathrm{synBCt}}, & \text{if } C_{\mathrm{synBCt}} > 0 \\ C_{\mathrm{synBCt}}, & \text{otherwise} \end{cases} \tag{A5b}$$

A part of syn_B (eq. A10), the C balance for biomass synthesis is used for catabolic growth respiration r_G to support biomass synthesis and the remaining fraction ϵ, the anabolic carbon use efficiency, is used for synthesis of biomass and enzymes. ϵ is assumed to be the equal for all substrates for simplicity. SESAM assumes that requirements for maintenance and enzyme synthesis must be met first. Therefore, the microbial C balance can become negative resulting in starvation and decline of microbial biomass.

$$\mathrm{r}_G = \begin{cases} \frac{1-\epsilon}{\epsilon}\,\mathrm{syn}_B, & \text{if } \mathrm{syn}_B > 0 \\ 0, & \text{otherwise}\,, \end{cases} \tag{A6a}$$

where syn_B is the C balance for biomass synthesis is given below by eq. A10.

A2 Nitrogen dynamics

Nitrogen fluxes are computed by dividing the respective C fluxes (A1) by the C/N ratio, β_N, of their source.

We assumed fixed C/N ratios $\beta_{N\,B}$ and $\beta_{N\,Enz}$ of the microbial biomass and enzymes. However, substrate N pools are modeled explicitly because their C/N ratio of the substrate pools may change over time.

$$\frac{dL_N}{dt} = -\,\mathrm{dec}_L/\beta_{N\,L} + \mathrm{i}_L(t)/\beta_{N\mathrm{i}} \tag{A7a}$$

$$\frac{dR_N}{dt} = -\,\mathrm{dec}_R/\beta_{N\,R} + \epsilon_{\mathrm{tvr}}\,\mathrm{tvr}_B/\beta_{N\,B} + (1-\kappa_E)\,\mathrm{syn}_{\mathrm{Enz}}/\beta_{N\,E} \tag{A7b}$$

$$u_{Plant,N} = min\,(u_{Plant,N,max}(t), k_{PlantN}(t)I) \tag{A7c}$$

$$\frac{dI_N}{dt} = +i_{I_N}(t) - u_{Plant,N} - l_N I_N + \Phi_N \tag{A7d}$$

$$\Phi_N = \Phi_{Nu} + \Phi_{NB} + r_{\mathrm{tvr}}/\beta_{N\,B} \tag{A7e}$$

$$\Phi_{Nu} = (1-\nu_N)u_{N,OM}, \tag{A7f}$$

The inorganic N pool I_N balances external inputs i_{I_N}, leaching $l_N I_N$, plant uptake u_{PlantN}, and the exchange flux with soil microbial biomass, Φ_N (Fig. A1).

https://doi.org/10.5194/egusphere-2022-359
Preprint. Discussion started: 4 July 2022

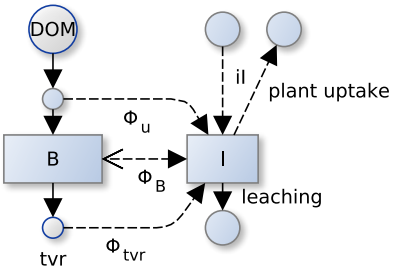

Figure A1. Several component fluxes sum to total mineralization flux in SESAM: $\Phi = \Phi_u + \Phi_B + \Phi_{\mathrm{tvr}}$. A negative mineralization flux, Φ_B corresponds to N immobilization of inorganic pool, I, by microbial biomass, B. In addition there is mineralization during microbial turnover, Φ_{tvr}, and mineralization during uptake, Φ_u. Fluxes across the system boundary are inputs of inorganic N, iI, inputs of organic N with litter, plant uptake of inorganic N, and leaching.

In addition to the mineralization-immobilization imbalance flux, Φ_{NB} (A11c), microbes exchange N with the inorganic pools by apparent mineralization due to soil heterogeneity, Φ_{Nu} (Manzoni et al., 2008) and mineralization of a part of microbial turnover, $r_{\mathrm{tvr}}/\beta_{NB}$ (A16, section A5).

Potential N uptake by microbes, $u_{N,Pot}$ (A8), is the sum of effective organic N uptake and potential inorganic uptake. The parallel scheme (PAR) (Manzoni et al., 2008) is used to model effective organic uptake. It accounts for an apparent mineralization at soil core scale caused by sub-scale soil spots with high N concentration in DOM. With PAR a part of the total organic N uptake, $(1-\nu_N)u_{N,OM}$, is mineralized. Uptake from DOM, $u_{N,OM}$, equals the influxes to DOM multiplied by the apparent N use efficiency ν_N.

$$u_{N,Pot} = \nu_N u_{N,OM} + u_{\mathrm{immN,Pot}} \tag{A8a}$$

$$u_{N,OM} = \mathrm{dec}_L/\beta_{NL} + \mathrm{dec}_R/\beta_{NR} + \kappa_E\,\mathrm{syn}_{\mathrm{Enz}}/\beta_{NEnz} \tag{A8b}$$

$$u_{\mathrm{immN,Pot}} = i_{BN} I_N, \tag{A8c}$$

where C/N ratios β_{NL} and β_{NR} are calculated using current C and N substrate pools: $\beta_{NL} = L/L_N$. Note that u_N is the potential microbial N uptake using the potential immobilization flux. The actual net inorganic flux, Φ_{NB}, is computed taking other limitation into account (A11c).

The N constraint on biomass synthesis is potential microbial N uptake minus enzyme synthesis. Converted to C units this reads: $C_{\mathrm{synB}} \le \beta_{NB} N_{\mathrm{synBN}}$.

$$N_{\mathrm{synBN}} = u_{N,Pot} - \mathrm{syn}_{\mathrm{Enz}}/\beta_{NEnz}, \tag{A9a}$$

https://doi.org/10.5194/egusphere-2022-359
Preprint. Discussion started: 4 July 2022

A3 Imbalance fluxes of microbes limited by C or N

There is a constraint on the synthesis of new biomass by each chemical element. In SESAM synthesis follows the minimum of these constraints (eq. A10).

$$\mathrm{syn}_B = min(C_{\mathrm{synBC}}, \beta_{NB} N_{\mathrm{synBN}}) \tag{A10}$$

The elements in excess then are lost by imbalance fluxes (eq. A11), so that the mass balance is closed. Excess N is mineralized (M_{Imb}), and excess C is respired by overflow respiration (r_O).

$$r_O = u_C - (\mathrm{syn}_B + \mathrm{r}_G + \mathrm{syn}_{\mathrm{Enz}}/\epsilon + r_M) \tag{A11a}$$

$$M_{\mathrm{ImbN}} = u_N - (\mathrm{syn}_B/\beta_{NB} + \mathrm{syn}_{\mathrm{Enz}}/\beta_{NEnz}) \tag{A11b}$$

$$\Phi_{EB} = M_{\mathrm{ImbE}} - u_{\mathrm{immE,Pot}} \tag{A11c}$$

The actual mineralization-immobilization flux Φ_{EB} for element E is the difference between excess mineralization of E and the potential immobilization flux. With substrate N limitation, Φ_{NB} will be negative (N immobilization), whereas if microbes are limited by C availability, Φ_{NB} will be positive (N mineralization). If required immobilization is larger than potential immobilization ($-\Phi_{NB} > u_{\mathrm{immN,Pot}}$) then stoichiometry must be balanced by overflow respiration.

A4 Community composition

Microbes in SESAM allocate a proportions α_Z of their total enzyme investments to the synthesis of enzyme Z. These enzyme allocation coefficient, α_Z, reflect the community composition, i.e. the mix of species growing on different portions of the organic matter.

SESAM models composition, α_Z, as a vector of state variables that develop over time towards the optimal composition, α_{ZOpt}. The time scale of this change is assumed to be equal to the timescale of microbial turnover, τ, and biomass synthesis, syn_B (A12).

$$\frac{d\alpha_Z}{dt} = (\alpha_{\mathrm{ZOpt}} - \alpha_Z)(\tau + |\mathrm{syn}_B|/B) \tag{A12}$$

Community can change fast if either its growing fast, of if its decaying fast. Hence, both terms are considered in (A12).

SESAM3 adopts the revenue strategy where investment into enzyme synthesis is proportional to its revenue (Wutzler et al., 2017). It differs from SEAM by considering the weights also in the computation of the investment.

https://doi.org/10.5194/egusphere-2022-359
Preprint. Discussion started: 4 July 2022

$$\alpha_{ZOpt} = \frac{\mathrm{rev}_Z}{\sum_\zeta \mathrm{rev}_\zeta} \approx \frac{\mathrm{rev}^*_Z}{\sum_\zeta \mathrm{rev}^*_\zeta} \tag{A13a}$$

$$\mathrm{rev}^*_Z = \frac{\text{limitation-weighted return}}{\text{limitation-weighted investment}} \tag{A13b}$$

$$\mathrm{investment}^*_Z = \alpha_Z a_E B(w_C + w_N/\beta_{N\,Enz}) \tag{A13c}$$

$$\begin{aligned}\mathrm{return}^*_Z &= \sum_E \mathrm{return}^*_{ZE}\, w_E \\ &= (w_C + w_N/\beta_{N\,Z})\,\mathrm{dec}_{Z_B}\,,\end{aligned} \tag{A13d}$$

α_Z is the current community enzyme allocation, rev_Z is the revenue from given enzyme depolymerizing substrates $Z \in \{L, R\}$ of organic matter and rev^*_Z its version computed with enzymes assumed in steady state. dec_{Z_B} is the decomposition due to biomass-produced enzymes (A3). The elemental limitation weights,w_E, occur in both the return and the investment, therefore they do not need to be normalized to one.

$$\mathrm{rev}^*_Z = \frac{k_Z Z}{k_{mN} + \alpha_Z a_E B} \frac{w_C + w_N/\beta_{N\,Z}}{w_C + w_N/\beta_{N\,Enz}} \tag{A14}$$

The unnormalized weight of an element limitation, w_E, decreases exponentially with the excess of biosynthesis flux constrained by the given element only over the actual biosynthesis flux constrained by all elements. This excess in potential biosynthesis flux is normalized by microbial turnover in order to derive a unitless quantity. Compared to the SEAM version 2 formulation of weights (Wutzler et al., 2017), this formulation works better for starving microbial community with negative biomass synthesis and can be extended to more than two limiting elements.

$$w_\mathrm{E} = \exp\left(-\delta \frac{C_\mathrm{synBE} - \mathrm{syn}_B}{\mathrm{tvr}_B}\right), \tag{A15}$$

where δ, arbitrarily set to 40, controls the steepness of the transition between states limited by different elements. C_synBE denotes the available biosynthesis flux in microbial biomass carbon equivalents given the limitation of element E (A5), (A9), e.g. for Nitrogen: $C_\mathrm{synBN} = \beta_{N\,B} N_\mathrm{synBN}$.

Compared with the SEAM, already a small C limitation causes an increased preference for the C-rich labile pool, i.e. lower α_R. This is because the elemental N limitation is divided by C/N ratio in (A13).

A5 Fate of microbial turnover

during microbial turnover a part $(1 - \epsilon_\mathrm{tvr})$ of microbial biomass is mineralized, e.g. by grazing.

$$r_\mathrm{tvr} = (1 - \epsilon_\mathrm{tvr})\,\mathrm{tvr}_B \tag{A16}$$

Respective proportion of N ($r_\mathrm{tvr}/\beta_{N\,B}$) is also mineralized and transferred to the inorganic N pools.

https://doi.org/10.5194/egusphere-2022-359
Preprint. Discussion started: 4 July 2022

The remainder of the microbial turnover goes to the residue pool. Current SESAM version ignores the part that enters the DOM pool and is taken up again by living microbial biomass. This corresponds to an effective uptake rate, assuming that the effects of this DOM flux on pools cancel in their parameterizations. This shortcut leads to a joint small underestimation of microbial turnover, uptake, and CUE. Investigating the effect of this simplifying assumption on isotopic tracers is an outlook.

Appendix B: Alternative return of microbial uptake

Instead of taking the entire decomposition flux as return, one could account for the mineralization-immobilization pathway and that during this path, part of the decomposition flux routed away from microbial biomass.

$$\mathrm{return}_{ZE} = \mathrm{dec}_{SZ}\,\nu_{TE} \tag{B1a}$$

$$\nu_{TE} = \nu_E + (1-\nu_E)p_{\mathrm{immo,E}} \tag{B1b}$$

where ν_{TE} is the total nutrient efficiency that includes the uptake by mineralization-immobilization pathway, $p_{\mathrm{immo,E}}$ is the ratio of microbial uptake from the pool of the inorganic form of the element E to the sum of all losses from this pool.

This leads to updated equations of return, revenue, and community composition (B2).

$$\mathrm{return}^*_S = \mathrm{dec}_{S_B}(w_C + w_N\nu_{TN}/\beta_{NS}), \tag{B2}$$

Notice, that ν_{TM} depends by $p_{\mathrm{immo,E}}$ on many aspects of the current state. This makes reasoning about the system more difficult.

When one element is clearly limiting, the sum across weights in the computation of α_Z, both in the return as numerator well in the denominator is dominated by only a single term. In this case the ν_{TN} cancels and the computed α_Z (A13a) equals the version computed by adopting the decomposition flux as return.

We argue that the case of clear co-limitation is quite rare. Depending on fluctuations in litter input and soil heterogeneity, the community at a given time and a given spot the microbial community is usually limited by one of the elements. Therefore, SESAM currently adopts the simpler version of the return (A13).

Appendix C: Robustness of sensitivity parameters

Results of repeated sensitivity analysis on a larger parameter subspace (Fig. C1) were very similar to the original sensitivity analysis (Fig. 5)

https://doi.org/10.5194/egusphere-2022-359
Preprint. Discussion started: 4 July 2022

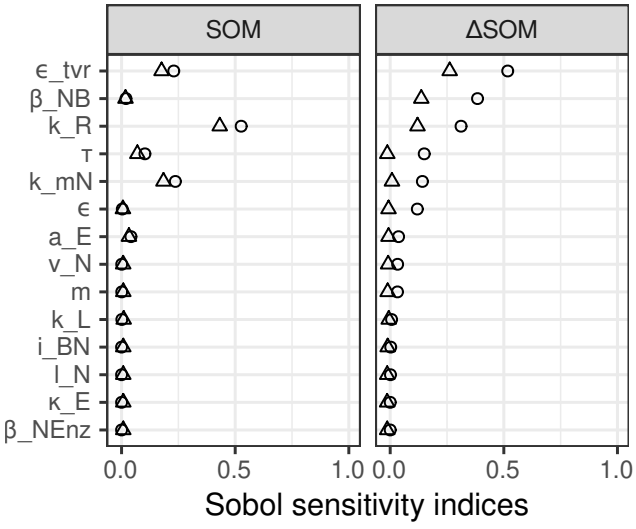

Figure C1. Modification of Fig 5 for sensitivity analysis repeated on larger subspace encompassing 40% of parameter ranges.

Appendix D: Supplementary figures of the fluctuation analyis

The following figures help to understand the result of section (3.4) that enzyme steady state assumptions did not introduce bias in predictions despite the non-linearity of decomposition with enzyme levels.

The aboveground litter inputs in autumn caused time-lagged responses and smoothed responsed in the modeled soil properties (Fig. D1). This smoothing behaviour is simililar to a daily temperature signal traveling down form top soil to deeper soil layers where the signal is delayed and smoothed.

Due to this smoothing and lagging behaviour, the simulated steady state enzyme levels closely tracked the explicit enzyme levels (Fig. D2).

Appendix E: No mass flux by enzymes

SESAM does not explicitly represent enzyme pools. However, the mass fluxes across the enzyme pool from biomass to DOM and to the residue pool are represented.

A model variant "NoEnzFlux" has been implemented, where the enzyme pools are still part of the revenue computation, but mass fluxes across the enzyme pools are neglected. This has been accomplished by using $syn_{Enz} = 0$ instead of (A2a) and using $a_E B$ directly in revenue computation (A13).

https://doi.org/10.5194/egusphere-2022-359
Preprint. Discussion started: 4 July 2022

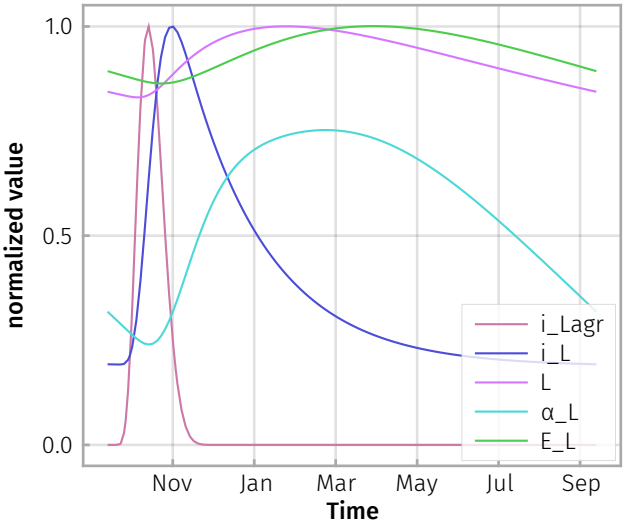

Figure D1. Model responses to a spike of aboveground litter fall in autumn, i_{Lagr} are damped. There is a cascade of delays in litter input from litter layer and roots to soil, i_L, change in litter substrate pool, L, increased share of microbial community depolymerizing this pool, α_L, and an increase in enzyme concentration, E_L. All fluxes were normalized by dividing by their maximum, unless α_L, whose range additionally was scaled to 0.5, because it varied only marginally across seasons.

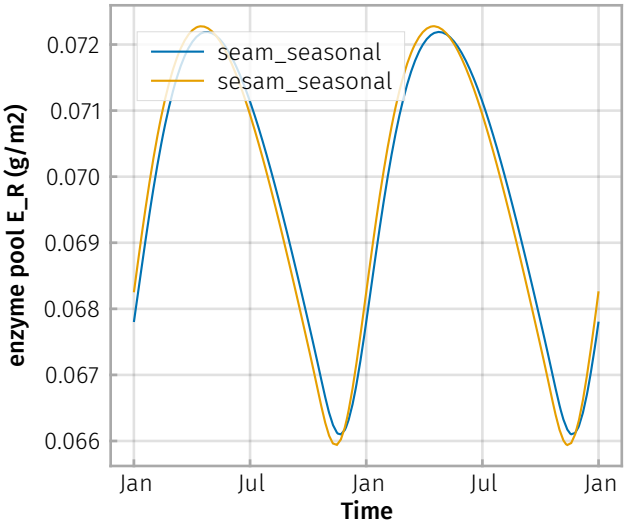

Figure D2. Enzyme levels, here shown for residue degrading enzyme, E_R, differ only marginally across simulations of explicit enzymes (seam) and steady state enzymes (sesam).

https://doi.org/10.5194/egusphere-2022-359
Preprint. Discussion started: 4 July 2022

Appendix F: Steady State of Microbial biomass

Here we derive equations for microbial biomass in quasi steady state.

With setting $dB = 0$: $\mathrm{syn}_B = \mathrm{tvr}_B$.

Carbon available for biomass synthesis, syn_B is the minimum for each element at limitation, either by C or by N. Hence, we compute the steady state biomass for all limitations and then take the minimum: $B_s = min(B_{sC}, B_{sN})$.

F1 Carbon limitation

With enzymes in quasi-steady-state, the uptake from enzyme turnover equals enzyme production, $a_E B$. While enzyme investments are subtracted from uptake for computing biomass synthesis, a part κ_E occurs in uptake.

$$\epsilon C_{\mathrm{syn}\,BC} = \tau B \tag{F1a}$$

$$u_C - \mathrm{syn}_E/\epsilon - r_M = \tau/\epsilon B \tag{F1b}$$

$$\frac{d_L(1-\alpha)a_E B}{k_{mN} + (1-\alpha)a_E B} + \frac{d_R \alpha a_E B}{k_{mN} + \alpha a_E B} + \kappa_E a_E B - \frac{a_E B}{\epsilon} - mB = \tau/\epsilon B \tag{F1c}$$

$$d_L(1-\alpha)a_E(k_{mN} + \alpha a_E B) + d_R \alpha a_E(k_{mN} + (1-\alpha)a_E B) = [\tau/\epsilon + m + (1/\epsilon - \kappa_E)a_E]\, c_1 \tag{F1d}$$

with abbreviations

$$d_L = dec_{L,Pot} = k_L L \tag{F2a}$$

$$d_R = dec_{R,Pot} = k_R R \tag{F2b}$$

$$c_1 = (k_{mN} + (1-\alpha)a_E B)(k_{mN} + \alpha a_E B) \tag{F2c}$$

$$\tau_{\epsilon m} = \tau/\epsilon + m + (1/\epsilon - \kappa_E)a_E \tag{F2d}$$

This results in square equation. If there is no real positive solution, biomass cannot be sustained, otherwise the maximum of the two roots gives the required steady state biomass, B_{sC}.

$$0 = aB^2 + bB + c \tag{F3a}$$

$$a = -\tau_{\epsilon m}\alpha(1-\alpha)a_E^2 \tag{F3b}$$

$$b = a_E^2 \alpha(1-\alpha)(d_L + d_R) - \tau_{\epsilon m} k_{mN} a_E \tag{F3c}$$

$$c = k_{mN} a_E\,[(1-\alpha)d_L + \alpha d_R] - \tau_{\epsilon m} k_{mN}^2 \tag{F3d}$$

F2 Nitrogen limitation

For N limitation, the potential immobilization flux does not cancel, and a complex cubed polinomial equations results.

https://doi.org/10.5194/egusphere-2022-359
Preprint. Discussion started: 4 July 2022

$$\epsilon C_{\mathrm{syn}\,BN} = \tau B \tag{F4a}$$

$$N_{\mathrm{syn}\,BN} = \tau B/\beta_B \tag{F4b}$$

$$\nu_N\left(dec_L/\beta_L + dec_R/\beta_R + \kappa_E\,\mathrm{tvr}_E/\beta_E\right) + u_{imm,Pot} - \mathrm{syn}_E/\beta_E = \tau B/\beta_B \tag{F4c}$$

$$\frac{d_{LN}(1-\alpha)a_E B}{k_{mN}+(1-\alpha)a_E B} + \frac{d_{RN}\alpha a_E B}{k_{mN}+\alpha a_E B} + \frac{\kappa_E a_E B}{\beta_E} + \frac{u_{imm,Pot}}{\nu_N} - \frac{a_E B}{\nu_N \beta_E} = \frac{\tau}{\nu_N \beta_B} B \tag{F4d}$$

$$d_{LN}(1-\alpha)a_E B(k_{mN}+\alpha a_E B) + d_{RN}\alpha a_E B(k_{mN}+(1-\alpha)a_E B) + u_{\nu N}c_1 = \tau_N B c_1 \tag{F4e}$$

with abbreviations

$$\tau_N = \frac{\tau}{\nu_N \beta_B} + \left(\frac{1}{\nu_N} - \kappa_E\right)\frac{a_E}{\beta_E} \tag{F5a}$$

$$u_{\nu N} = u_{imm,Pot}/\nu_N \tag{F5b}$$

$$d_{LN} = dec_{L,Pot}/\beta_L \tag{F5c}$$

$$d_{RN} = dec_{R,Pot}/\beta_R \tag{F5d}$$

$$c_1 = (k_{mN}+(1-\alpha)a_E B)(k_{mN}+\alpha a_E B) \tag{F5e}$$

This results in cubic equation. Its second root is real and gives the steady state biomass, B_{sN}.

$$0 = aB^3 + bB^2 + cB + d \tag{F6a}$$

$$a = -\tau_N \alpha(1-\alpha)a_E^2 \tag{F6b}$$

$$b = a_E^2\alpha(1-\alpha)\left(d_{LN}+d_{RN}+u_{\nu N}\right) - \tau_N k_{mN} a_E \tag{F6c}$$

$$c = a_E k_{mN}\left((\alpha-1)d_{LN} + \alpha d_{RN} + u_{\nu N}\right) - \tau_N k_{mN}^2 \tag{F6d}$$

$$d = k_{mN}^2 u_{\nu N} \tag{F6e}$$

(F6f)

While steady state biomass can be computed and passed to other equations that involve biomass, these other equations are not simplified.